J|A|C|S
ARTICLES
Published on Web 04/01/2004

Nature of Nonbonded Se···O Interactions Characterized by ^{17}O NMR Spectroscopy and NBO and AIM Analyses

Michio Iwaoka,*,† Hiroto Komatsu, Takayuki Katsuda, and Shuji Tomoda*

Contribution from the Department of Life Sciences, Graduate School of Arts and Sciences, The University of Tokyo, Komaba, Meguro-ku, Tokyo 153-8902, Japan

Received January 16, 2004; E-mail: miwaoka@keyaki.cc.u-tokai.ac.jp; tomoda@selen.c.u-tokyo.ac.jp

Abstract: To investigate the nature of nonbonded Se···O interactions, three series of 2-substituted benzeneselenenyl derivatives [2-(CHO)C_6H_4SeX (**1**), 2-(CH_2OH)C_6H_4SeX, (**2**), 2-(CH_2O*i*Pr)C_6H_4SeX (**3**); X = Cl, Br, CN, SPh, SeAr, Me] were synthesized. The ^{17}O NMR absorption observed for ^{17}O-enriched aldehydes **1** appeared upfield relative to benzaldehyde (PhCHO), while the opposite downfield shifts relative to benzyl alcohol (PhCH_2OH) were observed for ^{17}O-enriched alcohols **2** and ethers **3**. The magnitude of both the upfield and the downfield shifts became larger as the electron-withdrawing ability of a substituent X increased. Quantum chemical calculations at the B3LYP level revealed that for all model compounds the most stable conformer has an intramolecular nonbonded Se···O interaction. Thus, the relative ^{17}O NMR chemical shifts ($\Delta\delta_O$) for **1**−**3** would reflect the strengths of the Se···O interactions. The natural bond orbital (NBO) analysis demonstrated that the stabilization energy due to an $n_O \rightarrow \sigma^*_{Se-X}$ orbital interaction ($E_{Se\cdots O}$) correlates with the Se···O atomic distance on a single curve irrespective of the type of the O atom. On the other hand, the atoms in molecules (AIM) analysis showed that the nonbonded Se···O interactions can be characterized by the presence of a bond critical point, the total energy density ($H_{Se\cdots O}$) of which decreases with strengthening of the interaction. The results suggested that Se···O interactions have a dominant covalent character rather than an electrostatic one.

Introduction

Weak nonbonded interactions are useful chemical tools for controlling stability, conformation, and assembly of molecules.[1] It is, therefore, of great interest to determine the strengths and directional propensities of such interactions at an atomic resolution. However, detection as well as characterization of nonbonded interactions in situ is still challenging research in fundamental chemistry.[2] In this paper, we have extensively studied the nature of nonbonded interactions between a divalent selenium (Se) and an oxygen (O) atom, that is, Se···O interactions,[3] by means of experimental ^{17}O NMR spectroscopy and theoretical natural bond orbital (NBO)[4] and atoms in molecules (AIM)[5] analyses using three series of model compounds (**1**−**3**) (Chart 1).

Organoselenium compounds frequently possess unique chemical reactivities[6] and biological activities.[7] We are interested in physicochemical characterization of nonbonded interactions involving Se [e.g., Se···N,[8] Se···O,[3] Se···F,[9] and Se···X (X = Cl and Br)[10] interactions] in relation to their applications to asymmetric synthesis,[11,12] enzyme-mimetic reactions,[13] and protein engineering.[14] The nature of Se···O interactions has been most frequently studied in the literature.

Chart 1

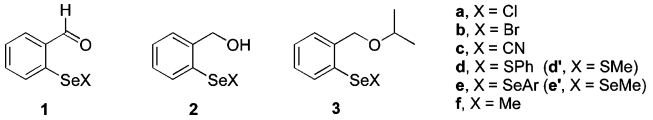

† Present address: Department of Chemistry, School of Science, Tokai University, Kitakaname, Hiratsuka-shi, Kanagawa 259-1292, Japan.

(1) (a) Israelachvili, J. *Intermolecular and Surface Forces*; Academic Press: London, 1991. (b) *Molecular Interactions*; Scheiner, S., Ed.; John Wiley and Sons: Chichester, 1997.
(2) Müller-Dethlefs, K.; Hobza, P. *Chem. Rev.* **2000**, *100*, 143−167.
(3) Komatsu, H.; Iwaoka, M.; Tomoda, S. *Chem. Commun.* **1999**, 205−206.
(4) Reed, A. E.; Curtiss, L. A.; Weinhold, F. *Chem. Rev.* **1988**, *88*, 899−926.
(5) (a) Bader, R. F. W. *Atoms in Molecules: A Quantum Theory*; Oxford University Press: New York, 1990. (b) Popelier, P. *Atoms in Molecules: An Introduction*; Pearson Education: Harlow, 2000. (c) Gillespie, R. J.; Popelier, P. L. A. *Chemical Bonding and Molecular Geometry*; Oxford University Press: New York, 2001.
(6) (a) *Organoselenium Chemistry: A Practical Approach*; Back, T. G., Ed.; Oxford University Press: New York, 1999. (b) *Organoselenium Chemistry: Modern Developments in Organic Synthesis*; Wirth, T., Ed.; Springer-Verlag: Berlin, 2000.
(7) (a) *Selenium in Biology and Human Health*; Burk, R. F., Ed.; Springer-Verlag: New York, 1994. (b) *Selenium. Its Molecular Biology and Role in human Health*; Hatfield, D. L., Ed.; Kluwer Academic Publishers: Boston, 2001.
(8) (a) Iwaoka, M.; Tomoda, S. *Phosphorus, Sulfur Silicon Relat. Elem.* **1992**, *67*, 125−130. (b) Iwaoka, M.; Tomoda, S. *J. Am. Chem. Soc.* **1996**, *118*, 8077−8084.
(9) (a) Iwaoka, M.; Komatsu, H.; Tomoda, S. *Chem. Lett.* **1998**, 969−970. (b) Iwaoka, M.; Komatsu, H.; Katsuda, T.; Tomoda, S. *J. Am. Chem. Soc.* **2002**, *124*, 1902−1909.
(10) Iwaoka, M.; Katsuda, T.; Tomoda, S.; Harada, J.; Ogawa, K. *Chem. Lett.* **2002**, 518−519.
(11) (a) Fujita, K.; Iwaoka, M.; Tomoda, S. *Chem. Lett.* **1994**, 923−926. (b) Fujita, K.; Murata, K.; Iwaoka, M.; Tomoda, S. *Tetrahedron* **1997**, *53*, 2029−2048.
(12) (a) Fragale, G.; Wirth, T. *Eur. J. Org. Chem.* **1998**, 1361−1369. (b) Fragale, G.; Neuburger, M.; Wirth, T. *Chem. Commun.* **1998**, 1867−1868.
(13) (a) Iwaoka, M.; Tomoda, S. *J. Chem. Soc., Chem. Commun.* **1992**, 1165−1167. (b) Iwaoka, M.; Tomoda, S. *J. Am. Chem. Soc.* **1994**, *116*, 2557−2561. (c) Wirth, T.; Häuptli, S.; Leuenberger, M. *Tetrahedron: Asymmetry* **1998**, *9*, 547−550. (d) Mugesh, G.; Singh, H. B. *Chem. Soc. Rev.* **2000**, *29*, 347−357. (e) Mugesh, G.; Panda, A.; Singh, H. B.; Punekar, N. S.; Butcher, R. J. *J. Am. Chem. Soc.* **2001**, *123*, 839−850. (f) Back, T. G.; Moussa, Z. *J. Am. Chem. Soc.* **2002**, *124*, 12104−12105.

Baiwir et al.[15] unambiguously demonstrated structural features of Se···O interactions by solving the solid-state molecular structure of 2-formylbenzeneselenenyl bromide (**1b**), in which the carbonyl O atom coordinates intramolecularly to the Se atom in a short distance (2.305 Å) constituting a hypervalent linear O···Se−Br atomic alignment. Due to this thermodynamic assistance, the selenenyl bromide species (ArSeBr), which is normally highly labile, could endure during the time-consuming X-ray analysis. Chemical properties of an intramolecular 1,4-type Se···O interaction were studied by Goldstein et al.:[16] On the basis of X-ray and ^{77}Se NMR analyses of biologically active selenazofurin, it was found that the increase of a positive charge on Se strengthens the Se···O interaction, suggesting a significant contribution from the electrostatic interaction between the Se and O atoms to the stability of the attractive Se···O interaction. On the other hand, Barton et al.[17] investigated the intramolecular 1,5-type Se···O interaction of selenoiminoquinones in the solid state: On the basis of ab initio molecular orbital (MO) calculation results, the Se···O interaction was considered as a 3-center 4-electron bond in terms of the VSEPR model.[18]

Recently, Minyaev and Minkin[19] carried out high-level ab initio calculations on β-chalcogenovinylaldehydes (CHOCH═CHXR; X = S, Se, Te and R = H, Cl) and showed that the molecular structures are controlled by the intramolecular 1,5-type O → chalcogen coordination. The result was in accord with experimental observations.[15−17] However, Mó et al.[20] pointed out that such chalcogen···O interactions would compete with the X−H···O hydrogen bond in the case of X = Se and R = H. They further insisted, on the basis of the results from NBO and AIM analyses, that the electrostatic and dative (or covalent) components are entangled in the 1,5-type Se···O interaction. Thus, the nature of Se···O interactions is also controversial from a theoretical point of view.

Meanwhile, Se···O interactions have been successfully applied to asymmetric oxyselenenylation reactions of olefins using chiral selenium reagents.[12] The achievement of efficient asymmetric induction was theoretically explained by assuming a credit of intramolecular Se···O interactions.[21] However, it is practically not easy to characterize Se···O interactions in the reaction solution. Therefore, the development of a simple experimental method to diagnose the chemical nature and the strength of Se···O interactions in situ would be useful for the design of more effective chiral selenium reagents or other functional selenium compounds.

In our previous report on nonbonded Se···O interactions,[3] ^{77}Se and ^{17}O NMR chemical shifts (δ_{Se} and δ_O) were shown to be sensitive to the presence of Se···O interactions by using a series of model compounds **1** and **2**. Although direct nuclear spin coupling (J) was not observed between the ^{77}Se and ^{17}O nuclei because of the quadrupolar nature of an ^{17}O nucleus, both ^{77}Se and ^{17}O NMR chemical shifts (δ_{Se} and δ_O) must be promising candidates as a probe for the nature of Se···O interactions. Herein, to demonstrate that the δ_O value can be applied as a good experimental measure for the strength of the Se···O interaction, we have analyzed quantitative behaviors of the δ_O values observed for **1**−**3** by fitting them to the theoretically available parameter, that is, the atomic distance between the Se and O atoms ($r_{Se\cdots O}$). In addition, the second-order perturbation energy due to the $n_O \rightarrow \sigma^*_{Se-X}$ orbital interaction ($E_{Se\cdots O}$) obtained by NBO analysis[4] and the total energy density of the bond critical point ($H_{Se\cdots O}$) obtained by AIM analysis[5] have been analyzed to investigate the stabilization mechanism. The results suggested that the Se···O interactions of **1**−**3** have a dominant covalent character rather than an electrostatic one.

Scheme 1

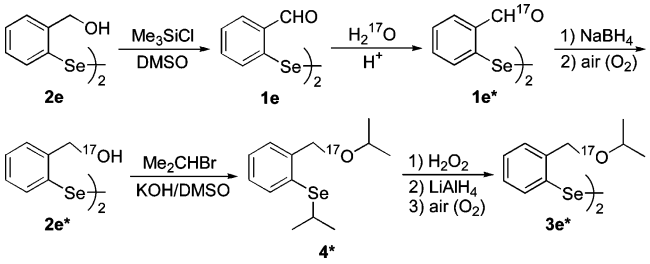

Results and Discussion

Synthesis of Model Compounds. ^{17}O-labeled **1**−**3** were synthesized by using ca. 22% ^{17}O-enriched water ($H_2{}^{17}O$) as the isotope source. According to Scheme 1, alcohol **2e**[8a] was oxidized to aldehyde **1e**, which subsequently allowed for an isotopic oxygen exchange reaction in the presence of an acid catalyst. Resulting **1e*** (i.e., **1e** enriched with ^{17}O) was reduced to **2e***. ^{17}O-enriched **3e*** was easily obtained from **2e*** by alkylation of the alcohol and diselenide groups to afford **4*** and the subsequent redox conversion to recover a diselenide linkage. Diselenides **1e***, **2e***, and **3e*** were transformed to the corresponding selenenyl chlorides (**a**, X = Cl), selenenyl bromides (**b**, X = Br), selenenyl cyanates (**c**, X = CN), selenenyl sulfides (**d**, X = SPh), and methyl selenides (**f**, X = Me) by applying common procedures.[8,9] All compounds were obtained in spectrally pure form except for **1d***, **2d***, and **3d***, which slowly disproportionated into the corresponding diselenides (**1e***, **2e***, and **3e***, respectively) at room temperature.

^{17}O and ^{77}Se NMR Chemical Shifts. The ^{17}O and ^{77}Se NMR chemical shifts (δ_O and δ_{Se}) observed for **1a**−**f**(*), **2a**−**f**(*), and **3a**−**f**(*) are listed in Table 1. On the basis of a similar discussion previously reported,[3] the presence of intramolecular Se···O interactions for these series of model compounds can be easily deduced from the NMR data.

First, δ_O values for **1** (δ_O = 493.0−561.6) were shifted upfield ($\Delta\delta_O$ = −76 to −7) as compared to that of reference compound benzaldehyde (PhCHO, δ_O = 569),[22] whereas δ_O values for **2** (δ_O = 24.9−10.6) and those for **3** (δ_O = 55.2−39.0) were

(14) (a) Iwaoka, M.; Takemoto, S.; Okada, M.; Tomoda, S. *Chem. Lett.* **2001**, 132−133. (b) Iwaoka, M.; Takemoto, S.; Okada, M.; Tomoda, S. *Bull. Chem. Soc. Jpn.* **2002**, *75*, 1611−1625. (c) Iwaoka, M.; Takemoto, S.; Tomoda, S. *J. Am. Chem. Soc.* **2002**, *124*, 10613−10620.
(15) Baiwir, M.; Llabres, G.; Dideberg, O.; Dupont, L.; Piette, J. L. *Acta Crystallogr.* **1975**, *B31*, 2188−2191.
(16) (a) Goldstein, B. M.; Kennedy, S. D.; Hennen, W. J. *J. Am. Chem. Soc.* **1990**, *112*, 8265−8268. (b) Burling, F. T.; Goldstein, B. M. *J. Am. Chem. Soc.* **1992**, *114*, 2313−2320.
(17) Barton, D. H. R.; Hall, M. B.; Lin, Z. Y.; Parekh, S. I.; Reibenspies, J. *J. Am. Chem. Soc.* **1993**, *115*, 5056−5059.
(18) (a) Gillespie, R. J.; Robinson, E. A. *Angew. Chem., Int. Ed. Engl.* **1996**, *35*, 495−514. (b) Gillespie, R. J. *Coord. Chem. Rev.* **2000**, *197*, 51−69.
(19) Minyaev, R. M.; Minkin, V. I. *Can. J. Chem.* **1998**, *76*, 776−788.
(20) (a) Sanz, P.; Yáñez, M.; Mó, O. *J. Phys. Chem. A* **2002**, *106*, 4661−4668. (b) Sanz, P.; Mó, O.; Yáñez, M. *Phys. Chem. Chem. Phys.* **2003**, *5*, 2942−2947.
(21) Spichty, M.; Fragale, G.; Wirth, T. *J. Am. Chem. Soc.* **2000**, *122*, 10914−10916.
(22) Boykin, D. W.; Baumstark, A. L. In *^{17}O NMR Spectroscopy in Organic Chemistry*; Boykin, D. W., Ed.; CRC Press: Boca Raton, FL, 1991; pp 205−231.

Table 1. ^{77}Se and ^{17}O NMR Chemical Shifts (δ_{Se} and δ_O) for **1**−**3**[a]

		1 (CHO)		**2** (CH_2OH)		**3** (CH_2O*i*Pr)	
	X	δ_{Se}[b]	δ_O[b]	δ_{Se}[b]	δ_O[b]	δ_{Se}	δ_O
a	Cl	1114.1	493.0	987.1	24.9	986.5	54.8
b	Br	1029.5	515.9	839.5	23.2	857.8	55.2
c	CN	426.7	548.0	314.5	22.0	315.1	44.6
d	SPh	621.7	556.6	501.8	16.0	503.8	44.4
e	SeAr	458.5	559.3	433.2	13.3	412.0	39.0
f	Me	259.5	561.6	157.2	10.6	166.6	39.0

[a] ^{77}Se NMR spectra were measured at 95.35 MHz in $CDCl_3$ at 298 K with Me_2Se as an external standard. ^{17}O NMR spectra were measured for the corresponding ^{17}O-enriched compounds at 67.70 MHz in $CDCl_3$ at 298 K with D_2O as an external standard. [b] Data from ref 3.

Chart 2

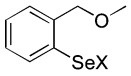

5

a, X = Cl
b, X = Br
c, X = CN
d', X = SMe
e', X = SeMe
f, X = Me

shifted downfield ($\Delta\delta_O$ = 24.2−9.9 and 54.5−38.3, respectively) as compared to that of reference compound benzyl alcohol ($PhCH_2OH$, δ_O = 0.7).[23] The observed opposite shifts were reasonably due to the different types of hybrid orbitals for the O atom of **1** (sp^2) and those of **2** and **3** (sp^3).[24] Second, the magnitudes of both the upfield and the downfield shifts became larger as the electron-withdrawing ability of a substituent X increased, that is, **a** (Cl) > **b** (Br) > **c** (CN) > **d** (SPh) > **e** (SeAr) > **f** (Me), except for the case of **3a** ($\Delta\delta_O$ = 54.1) and **3b** ($\Delta\delta_O$ = 54.5): The monotonic downfield shift of δ_O was observed for the series of compound **1** on going from **1a** to **1f** (δ_O = 493.0 → 561.6), while the opposite trend was apparent for the series of **2** (δ_O = 24.9 → 10.6) and **3** (δ_O = 55.2 → 39.0). Third, the ^{77}Se NMR absorptions (δ_{Se}) for **1a**−**f** were significantly shifted downfield from those for the corresponding **2a**−**f** and **3a**−**f**, suggesting the presence of strong magnetic anisotropic effects on the Se atoms of series **1a**−**f** from the intramolecular carbonyl group that must locate in close proximity to the Se atom.

Thus, the NMR data in Table 1 allowed us to suppose that the major conformer in solution for three series of model compounds (**1a**−**f**, **2a**−**f**, and **3a**−**f**) should be the one that has a close atomic contact between the Se and O atoms, that is, an intramolecular Se···O interaction.

Quantum Chemical Calculation. To assign the most stable molecular structure for each model compound (**1a**−**f**, **2a**−**f**, and **3a**−**f**) by theoretical calculation, a systematic conformer search, in which all possible values were applied for each changeable dihedral angle, was carried out at the HF/631H level (see Experimental Section for the abbreviation). The obtained stable structures were subsequently optimized without restrictions at the B3LYP/631H level. Simplified structures were employed for some model compounds to save the computation time. Isopropyl groups of **3a**−**f** were treated as methyl groups in **5a**−**f** (Chart 2). Phenylthio substituents (SPh) of **1d**, **2d**, and **3d** were altered to methylthio groups (SMe) in **1d′**, **2d′**, and **5d′**.

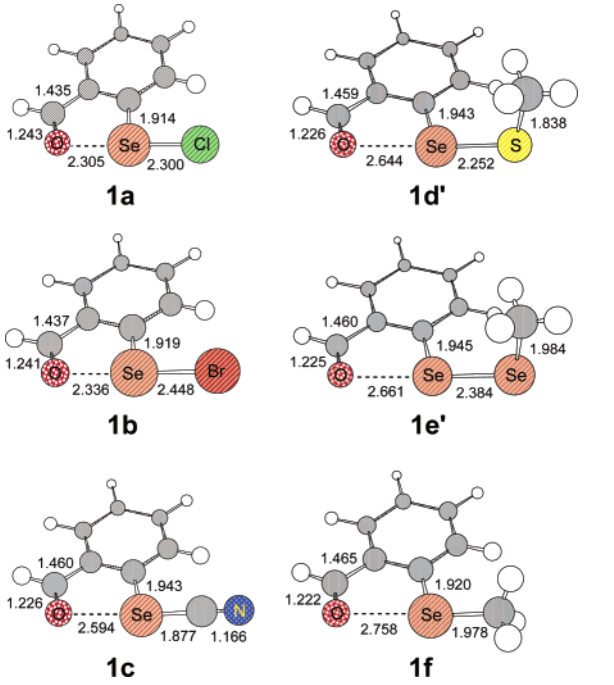

Figure 1. The most stable structures for **1a**−**f** obtained by quantum chemical calculation at the B3LYP/631H//B3LYP/631H level. The pertinent bond lengths are given in angstroms.

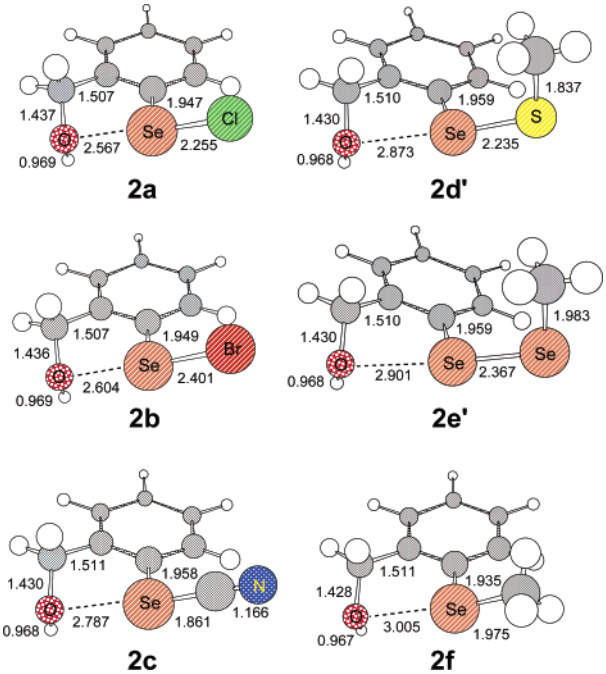

Figure 2. The most stable structures for **2a**−**f** obtained by quantum chemical calculation at the B3LYP/631H//B3LYP/631H level. The pertinent bond lengths are given in angstroms.

Similarly, arylseleno substituents (SeAr) of **1e**, **2e**, and **3e** were altered to methylseleno groups (SeMe) in **1e′**, **2e′**, and **5e′**. The simplification should not significantly affect the calculation results.

The most stable molecular structures obtained for **1a**−**f**, **2a**−**f**, and **5a**−**f** in vacuo at the B3LYP/631H level are shown in Figures 1−3, respectively. For each model compound, the conformer with an intramolecular Se···O interaction was found to be most stable. The relative stability to other stable conform-

(23) Balakrishnan, P.; Baumstark, A. L.; Boykin, D. W. *Tetrahedron Lett.* **1984**, *25*, 169−172.
(24) (a) Béraldin, M. T.; Vauthier, E.; Fliszár, S. *Can. J. Chem.* **1982**, *60*, 106−110. (b) Jaccard, G.; Carrupt, P. A.; Lauterwein, J. *Magn. Reson. Chem.* **1988**, *26*, 239−244.

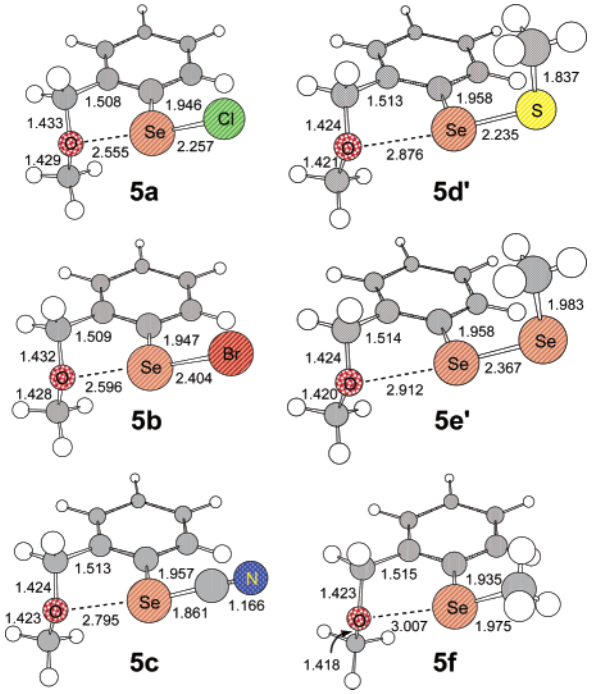

Figure 3. The most stable structures for **5a**−**f** obtained by quantum chemical calculation at the B3LYP/631H//B3LYP/631H level. The pertinent bond lengths are given in angstroms.

Table 2. Structural Parameters for 2-Formylbenzeneselenenyl Bromide (**1b**) Obtained by Quantum Chemical Calculation in Comparison to Those Determined by X-ray Crystallographic Analysis

atomic distance	B3LYP (Å)[a]	X-ray (Å)[b]	difference (Å)
Se−Br	2.448	2.403(4)	0.045
Se···O	2.336	2.305(19)	0.031
Se−C	1.919	1.876(19)	0.043
C═O	1.241	1.248(33)	−0.007
C−C	1.437	1.420(36)	0.017
C···C	1.401[c]	1.400[c]	0.001
angle	**B3LYP (deg)[a]**	**X-ray (deg)[b]**	**difference (deg)**
Br−Se···O	177.6	176.8	0.8
Br−Se−C	98.7	98.0(6)	0.7
O···Se−C	79.0	79.1(8)	−0.1
C═O···Se	107.1	106(2)	1
O═C−C	120.8	123(2)	−2
C−C···C_{Se}	117.1	113(2)	4
C−C···C_H	122.1	122(2)	0
Se−C···C_C	116.1	118(1)	−2
Se−C···C_H	125.4	126(2)	−1
C···C···C	120.0[c]	120[c]	0

[a] Optimized at the B3LYP/631H level. [b] Data from ref 15. [c] Averaged values.

ers that do not have an intramolecular Se···O interaction ranged from 3.0 to 11.6 kcal/mol for **1a**−**f**, 0.4 to 3.5 kcal/mol for **2a**−**f**, and 0.4 to 3.0 kcal/mol for **5a**−**f**.

Accuracy of the calculation results was confirmed by the good agreement between the molecular structure of **1b** obtained in silico and that determined by X-ray analysis.[15] Table 2 compares the structural parameters of **1b**. All atomic distances and angles of **1b** in the solid state are reasonably reproduced by the theoretical calculation at the B3LYP/631H level within the experimental errors, except that the atomic distances around the Se atom (i.e., Se−Br, Se···O, and Se−C) are slightly, but

Table 3. Summary of Quantum Chemical Calculations on **1a**−**f**, **2a**−**f**, and **5a**−**f** and the Natural Bond Orbital (NBO) Analysis[a]

comp	X	$r_{Se\cdots O}$ (Å)	$\theta_{O\cdots Se-X}$ (deg)	ω_{Ar-Se}[b] (deg)	ω_{Ar-C}[c] (deg)	q_{Se}[d] (e)	q_O[d] (e)	$E_{Se\cdots O}$[e] (kcal/mol)
1a	Cl	2.305	176.4	180.0	0.0	0.630	−0.551	36.07
1b	Br	2.336	177.6	180.0	0.0	0.538	−0.548	33.80
1c	CN	2.594	171.9	180.0	0.0	0.570	−0.542	11.33
1d′	SMe	2.644	176.4	178.5	0.6	0.390	−0.537	10.72
1e′	SeMe	2.661	177.4	178.5	0.5	0.302	−0.530	10.66
1f	Me	2.758	173.9	180.0	0.0	0.487	−0.536	6.19
2a	Cl	2.567	175.2	161.3	39.2	0.485	−0.739	14.80
2b	Br	2.604	175.7	159.7	40.8	0.401	−0.738	13.61
2c	CN	2.787	170.9	158.7	46.3	0.500	−0.753	5.95
2d′	SMe	2.873	174.5	157.6	49.4	0.308	−0.751	4.71
2e′	SeMe	2.901	175.1	156.9	50.8	0.222	−0.748	4.46
2f	Me	3.005	171.0	156.2	54.9	0.402	−0.751	2.57
5a	Cl	2.555	175.5	161.5	39.5	0.490	−0.566	14.38
5b	Br	2.596	175.9	159.9	41.2	0.404	−0.565	13.17
5c	CN	2.795	170.9	158.7	47.2	0.498	−0.578	4.86
5d′	SMe	2.876	175.2	159.3	49.5	0.310	−0.571	4.21
5e′	SeMe	2.912	175.2	157.4	51.5	0.218	−0.569	3.87
5f	Me	3.007	171.3	156.9	54.4	0.400	−0.571	2.26

[a] Selected structural parameters are shown for the most stable conformers (see Figures 1−3) obtained at the B3LYP/631H//B3LYP/631H level. NBO analysis was performed at the same calculation level. [b] The dihedral angle of the X−Se−C···C_C linkage. [c] The dihedral angle of the O−C−C···C_{Se} linkage. [d] The atomic charge of the selenium or oxygen atom determined by natural population analysis. [e] The orbital interaction energy between the oxygen lone pairs (n_O) and the antibonding orbital (σ^*_{Se-X}) determined by NBO second-order perturbation analysis.

significantly, shorter in the solid state than those in the calculated structure. The discrepancy may be due to intermolecular interactions in the solid state, as previously explained for the shrinking of hypervalent Br−Se−Br and Cl−Se−Cl fragments.[25] The potential surface of the hypervalent Br−Se···O fragment of **1b** should be so shallow, thereby so sensitive to the surrounding environment, that the fragment may be slightly shrunk in the solid state due to the crystal packing force.

Table 3 summarizes the structural parameters of the most stable conformers that were assigned for **1a**−**f** (Figure 1), **2a**−**f** (Figure 2), and **5a**−**f** (Figure 3) by quantum chemical calculation. Compounds **1a**−**f** possessed a planar structure according to the values of dihedral angles for the Se−X and C−O bonds with respect to the aromatic ring (i.e., ω_{Ar-Se} and ω_{Ar-C}, respectively), while distorted structures were obtained for **2a**−**f** and **5a**−**f** as seen in the values of ω_{Ar-Se} (156.2−161.5°) and ω_{Ar-C} (39.2−54.9°). The structural parameters for **2a**−**f** were very similar to those for **5a**−**f**, suggesting that the displacement of the hydroxy groups of **2a**−**f** with alkoxy groups in **5a**−**f** would make only marginal effects on the conformation. The apparently short atomic distances between Se and O atoms ($r_{Se\cdots O}$) relative to the sum of the van der Waals radii [vdw(Se) + vdw(O) = 1.90 + 1.52 = 3.42 Å][26] as well as the almost linear O···Se−X angles ($\theta_{O\cdots Se-X}$) clearly show the presence of a hypervalent Se···O interaction for all model compounds. It should be noted that $r_{Se\cdots O}$ was 0.1−0.3 Å longer when calculated at the HF/631H level.[3] Because the electron correlation is more sufficiently included in the B3LYP method than in the HF method, the observed shortening of $r_{Se\cdots O}$ at the B3LYP/631H level (Table 3) suggested the contribution from the electron correlation to the stability of the Se···O interactions.

(25) Iwaoka, M.; Komatsu, H.; Tomoda, S. *J. Organomet. Chem.* **2000**, *611*, 164−171.
(26) Bondi, A. *J. Phys. Chem.* **1964**, *68*, 441−451.

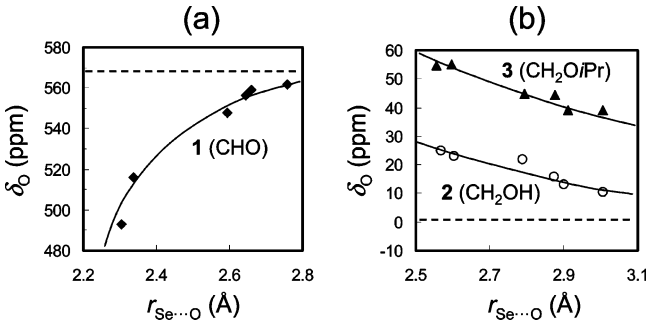

Figure 4. Correlation between the ^{17}O NMR chemical shifts (δ_O) and the Se···O atomic distances ($r_{Se\cdots O}$) calculated at the B3LYP/631H//B3LYP/631H level. (a) Correlation plots for **1a**−**f** (CHO). The dashed line indicates the ^{17}O NMR chemical shift for PhCHO ($\delta_O = 569$).[22] (b) Correlation plots for **2a**−**f** (CH_2OH) and **3a**−**f** (CH_2OiPr). The dashed line indicates the ^{17}O NMR chemical shift for $PhCH_2OH$ ($\delta_O = 0.7$).[23] The Se···O atomic distances ($r_{Se\cdots O}$) calculated for **5a**−**f** (CH_2OMe) are applied for **3a**−**f**.

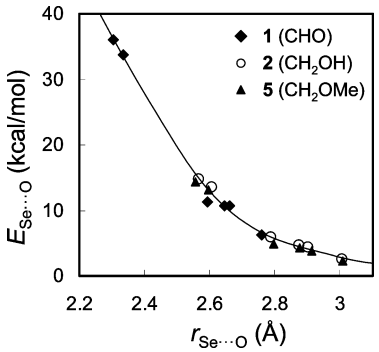

Figure 5. Correlation plots of the NBO second-order perturbation energies ($E_{Se\cdots O}$) versus the Se···O atomic distances ($r_{Se\cdots O}$) calculated at the B3LYP/631H//B3LYP/631H level. The solid curve is drawn for convenience.

Because the Se···O atomic distance ($r_{Se\cdots O}$) is a simple and unambiguous measure for the strength of Se···O interactions, their correlation to the ^{17}O NMR chemical shifts (δ_O) observed for **1a**−**f**, **2a**−**f**, and **3a**−**f** is plotted in Figure 4. It is seen that the shorter the Se···O atomic distance, the larger the upfield shift of ^{17}O NMR for **1a**−**f** relative to PhCHO (a dashed line in Figure 4a) and the larger the downfield shift of ^{17}O NMR for **2a**−**f** and **3a**−**f** relative to $PhCH_2OH$ (a dashed line in Figure 4b). The monotonic correlations demonstrated that the major conformer for **1a**−**f**, **2a**−**f**, and **3a**−**f** in the NMR solvent ($CDCl_3$) possesses an Se···O interaction and also that the strength of the Se···O interaction decreases on going from **a** (X = Cl) to **f** (X = Me) for all series of compounds.

Conformations of **1a**−**f**, **2a**−**f**, and **3a**−**f** in solution should be affected by the solvent effect, which generally tends to stabilize a more polar conformer than a less polar one due to more efficient solvation around the exposed polar surface. This implies that the conformer with an intramolecular Se···O interaction, which has the polar surface less exposed than other open conformers, would be destabilized in solution to some extent. According to the correlations shown in Figure 4, however, all model compounds should keep an intramolecular Se···O interaction in the NMR solution. This in turn indicates that the solvent effects on the conformations of **1a**−**f**, **2a**−**f**, and **3a**−**f** would be weak.

The atomic charges of Se and O atoms for **1a**−**f**, **2a**−**f**, and **5a**−**f** (q_{Se} and q_O in Table 3) suggest the significance of the electrostatic interaction between a positively charged Se atom and a negatively charged O atom for the stability of the Se···O interactions. However, the values of q_{Se} and q_O do not seem to correlate well with the strength (i.e., the trends of the ^{17}O NMR and the Se···O atomic distance), except for the monotonic tendency that the q_O values calculated for **1a**−**f** become less negative on going from **1a** to **1f**. In our previous calculation at the HF/631H level,[3] it was found that the higher the charge of the O atom, the larger the upfield shift of ^{17}O NMR for **1a**−**f** and the larger the downfield shift of ^{17}O NMR for **2a**−**f**. The calculation results at the B3LYP/631H level (Table 3) took over the trend observed at the lower calculation level (i.e., the HF/631H level) for **1a**−**f**, but not for **2a**−**f**. The considerations suggested that the nature of the Se···O interaction cannot solely be explained by the electrostatic interaction between Se and O atoms.

NBO Analysis. To evaluate the contribution from the orbital interaction between Se and O atoms to the stability of Se···O interactions, the NBO second-order perturbation analysis[4] was applied for the most stable conformers of **1a**−**f**, **2a**−**f**, and **5a**−**f** at the B3LYP/631H level. The obtained stabilization energies due to the $n_O \rightarrow \sigma^*_{Se-X}$ orbital interactions ($E_{Se\cdots O}$) are listed in the last column of Table 3. Because the O atom has two lone pairs of electrons, the $E_{Se\cdots O}$ values are indicated in the sum of the two possible $n_O \rightarrow \sigma^*_{Se-X}$ orbital interactions.

In the NBO analysis, natural bond orbitals are first defined for each covalent bond, lone pair, and antibonding orbital by using the molecular orbitals obtained by quantum chemical calculation, and the orbital interaction energies (i.e., the NBO second-order perturbation energies) are subsequently analyzed for all possible combinations of the two natural bond orbitals. Like Se···N[8] and Se···F[9] interactions, the orbital interactions between the O lone pairs (n_O) and the antibonding orbital of the Se−X bond (σ^*_{Se-X}) were found to contribute significantly to stabilization of the Se···O interactions: the $E_{Se\cdots O}$ values ranged from 6.19 to 36.07 kcal/mol for **1a**−**f**, 2.57 to 14.80 kcal/mol for **2a**−**f**, and 2.26 to 14.38 kcal/mol for **5a**−**f**.

The $n_O \rightarrow \sigma^*_{Se-X}$ orbital interaction energies ($E_{Se\cdots O}$) decrease on going from **a** (X = Cl) to **f** (X = Me) for all series. On the other hand, for the compounds with the same substituent X, **1** (CHO) has a much larger value of $E_{Se\cdots O}$ than **2** (CH_2OH), and **2** has approximately the same value of $E_{Se\cdots O}$ as **5** (CH_2OMe). The trends indicated the importance of the electrophilicity of the Se−X bond and the nucleophilicity of the O atom for the Se···O interactions. Because the observed trends are in complete agreement with the tendency of the Se···O atomic distance ($r_{Se\cdots O}$) calculated for **1a**−**f**, **2a**−**f**, and **5a**−**f**, the $n_O \rightarrow \sigma^*_{Se-X}$ orbital interaction mechanism reasonably explains the tendency of the strength of the Se···O interactions. The nice correlation between $E_{Se\cdots O}$ and $r_{Se\cdots O}$ (Figure 5) strongly suggests that the $n_O \rightarrow \sigma^*_{Se-X}$ orbital interaction is a major factor for the stability of the Se···O interactions. It is noteworthy that $E_{Se\cdots O}$ and $r_{Se\cdots O}$ exhibit a single correlation curve irrespective of the type of the O atom (i.e., whether it is involved in CHO, CH_2OH, or CH_2OR groups), while such a simple correlation is not present between the atomic charges of Se and O atoms (q_{Se} and q_O) and their atomic distance ($r_{Se\cdots O}$).

AIM Analysis. To investigate the nature of Se···O interaction from another point of view, atoms in molecules (AIM) analysis[5] was performed by using the calculation results at the B3LYP/631H level. In the AIM analysis, topological properties of the

Table 4. Bond Critical Point (BCP) Properties of Se···O Interactions for **1a**−**f**, **2a**−**f**, and **5a**−**f**[a]

comp	X	$\rho_{Se\cdots O}$[b] (ea_0^{-3})	$\nabla^2\rho_{Se\cdots O}$[c] ($ea_0^{-5}$)	$H_{Se\cdots O}$[d] (ea_0^{-4})
1a	Cl	0.053	0.130	−0.0053
1b	Br	0.050	0.124	−0.0045
1c	CN	0.030	0.084	−0.0002
1d′	SMe	0.028	0.077	−0.0002
1e′	SeMe	0.027	0.075	−0.0002
1f	Me	0.022	0.065	0.0002
2a	Cl	0.032	0.084	−0.0012
2b	Br	0.030	0.079	−0.0011
2c	CN	0.021	0.060	0.0001
2d′	SMe	0.018	0.051	0.0000
2e′	SeMe	0.018	0.049	0.0000
2f	Me	0.014	0.043	0.0003
5a	Cl	0.032	0.085	−0.0013
5b	Br	0.030	0.079	−0.0011
5c	CN	0.020	0.058	0.0002
5d′	SMe	0.018	0.050	0.0001
5e′	SeMe	0.017	0.048	0.0001
5f	Me	0.014	0.042	0.0004

[a] AIM analysis was performed for the most stable conformers (see Figures 1−3) obtained at the B3LYP/631H//B3LYP/631H level. [b] The electron density at the BCP. [c] The Laplacian of the electron density at the BCP. [d] The total energy density at the BCP.

electron density are analyzed to define the bond path between bonding (or interacting) atoms. Chemical bondings can be characterized by a so-called bond critical point (BCP), where the electron density becomes a minimum value along the bond path. For all Se···O interactions of model compounds (in the molecular structures shown in Figures 1−3), the BCP could be located. Table 4 summarizes the BCP properties of Se···O interactions for **1a**−**f**, **2a**−**f**, and **5a**−**f**.

The electron density (ρ) at a BCP correlates with the strength of an atomic interaction. The values of ρ obtained for the Se···O interactions of **1a**−**f**, **2a**−**f**, and **5a**−**f** ($\rho_{Se\cdots O}$) ranged from 0.014 to 0.053 ea_0^{-3}, which are remarkably lower than normal covalent bonds ($\rho_{C-C} \approx 0.24\ ea_0^{-3}$)[5b] but are significantly higher than the practical boundary of a molecule ($\rho \approx 0.001\ ea_0^{-3}$). The range was similar to that for neutral hydrogen bonds ($\rho_{H-bond} \approx 0.002-0.04\ ea_0^{-3}$),[5b] suggesting that the strength of the Se···O interactions competes with that of hydrogen bonds. The tendency that $\rho_{Se\cdots O}$ decreases in the order of **a** (X = Cl) > **b** (X = Br) > **c** (X = CN) > **d′** (X = SMe) > **e′** (X = SeMe) > **f** (X = Me) is in full accordance with the tendency of $E_{Se\cdots O}$ obtained by NBO analysis as well as $r_{Se\cdots O}$ obtained by quantum chemical calculation (see Table 3).

The Laplacian ($\nabla^2\rho_{Se\cdots O}$) represents the curvature of the electron density in three-dimensional space at the BCP of the Se···O interaction. In general, a negative value of $\nabla^2\rho$ indicates that the electron density is locally concentrated, while a positive value of $\nabla^2\rho$ means that the electron density is locally depleted. Therefore, the sign of $\nabla^2\rho$ at a BCP is considered to relate whether the atomic interaction possesses a dominant character of the shared electron (covalent) interactions ($\nabla^2\rho < 0$) or the closed-shell (electrostatic) interactions ($\nabla^2\rho > 0$). The values of $\nabla^2\rho_{Se\cdots O}$ listed in Table 4 are all positive, suggesting that the Se···O interactions have a dominant electrostatic character. Moreover, their magnitude decreases on going from **a** (X = Cl) to **f** (X = Me). The results are in conflict with the earlier discussion based on the NBO analysis (i.e., the tendency of $E_{Se\cdots O}$).

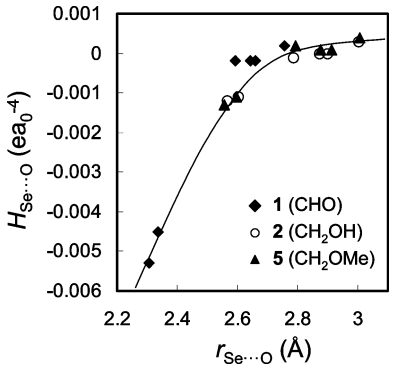

Figure 6. Correlation plots of the AIM total energy densities ($H_{Se\cdots O}$) versus the Se···O atomic distances ($r_{Se\cdots O}$) calculated at the B3LYP/631H//B3LYP/631H level. The solid curve is drawn for convenience.

However, it was previously pointed out that the total energy density (H) at a BCP, instead of the Laplacian, is a more appropriate index to approach better understanding of weak nonbonded interactions.[27] A total energy density (H) is given as a sum of two energy density terms; $H = G + V$, where G is the electronic kinetic energy density and V is the electronic potential energy density. When the value of H at a BCP is positive (i.e., $G > -V$), accumulation of electrons at the BCP is destabilizing. When the value of H at a BCP is negative (i.e., $G < -V$), accumulation of electrons at the BCP is stabilizing. Thus, within the framework of the AIM theory, the sign of H at the BCP assigns whether the interaction is electrostatic dominant ($H > 0$) or covalent dominant ($H < 0$). It should be noted that a covalent interaction in the AIM theory relates to an orbital interaction in the NBO analysis.

According to the values of $H_{Se\cdots O}$ listed in Table 4, it seems that the Se···O interactions have a dominant covalent character, although when the Se···O interaction is weak, the value of $H_{Se\cdots O}$ becomes slightly positive. Figure 6 shows the correlation plots between the total electron density at the BCP ($H_{Se\cdots O}$) and the atomic distance between the Se and O atoms ($r_{Se\cdots O}$). It is seen that $H_{Se\cdots O}$ becomes more negative with a decrease in the Se···O atomic distance (i.e., with strengthening of the Se···O interaction). The correlation, which is independent of the type of the O atom, supports the consideration that the Se···O interactions have a distinctly covalent nature rather than an electrostatic one.

Conclusions

As to the nature of Se···O interactions, both covalent and electrostatic characters should be important for the stability. However, NBO (i.e., $E_{Se\cdots O}$) and AIM (i.e., $H_{Se\cdots O}$) analyses presented in this paper strongly suggested that the $n_O \rightarrow \sigma^*_{Se-X}$ orbital interactions are dominantly important, although the Laplacian of the electron density at the bond critical point ($\nabla^2\rho_{Se\cdots O}$) suggested dominance of the electrostatic interaction between a positively charged Se and a negatively charged O atom. Because the total energy density ($H_{Se\cdots O}$) may be a better probe for characterization of weak interactions than the Laplacian,[27] it must be reasonable to conclude that the Se···O interactions for **1a**−**f**, **2a**−**f**, and **3a**−**f** have a dominant covalent character rather than an electrostatic one. This was also

(27) (a) Koch, W.; Frenking, G.; Gauss, J.; Cremer, D.; Collins, J. R. *J. Am. Chem. Soc.* **1987**, *109*, 5917−5934. (b) Rozas, I.; Alkorta, I.; Elguero, J. *J. Am. Chem. Soc.* **2000**, *122*, 11154−11161.

supported by the poor correlation observed between the tendency of the atomic charges of the Se and O atoms (q_{Se} and q_O, respectively) and the distance between the Se and O atoms (see Table 3). Meanwhile, the electron correlation was also suggested to be important for the Se···O interactions in addition to the covalent and electrostatic factors, according to significant elongation of the Se···O atomic distance in the HF structures,[3] which do not include the electron correlation sufficiently.

The above considerations are in accord with the nature of Se···N[8] and Se···F[9] interactions. Nonbonded Se···N and Se···F interactions have been clearly characterized by the observation of the nuclear spin−spin coupling between the interacting atoms, which gave clear evidence to the significance of the orbital interactions. As for Se···F interactions, the importance of the electron correlation has been additionally suggested for the stability. Because oxygen locates between nitrogen and fluorine in the periodic table of elements, it is quite consistent that Se···O interactions have an intermediate chemical character between Se···N and Se···F interactions.

From a practical point of view, it is important to develop a simple experimental method to determine the strength of Se···O interactions. The correlation shown in Figure 4 demonstrated that the ^{17}O NMR chemical shift (δ_O) is useful as the probe, but it is not always easy to observe ^{17}O NMR in laboratories unless the sample compound has been labeled with an ^{17}O nucleus. On the other hand, the correlations shown in Figures 5 and 6 strongly suggested that the Se···O interactions involving various types of an O atom can be treated as one class: the single correlation between the strength and the covalent character covers the range of the three types of Se···O interactions. The discovered correlations would be useful when the strength of the Se···O interaction is estimated from the Se···O atomic distance. Another possibility to apply the ^{77}Se NMR chemical shift (δ_{Se}) as a probe for the strength of Se···O interactions will be discussed in due course.

Experimental Section

General Procedures. Commercially available organic and inorganic reagents were used without further purification. Tetrahydrofuran (THF) was dried over sodium wire and was distilled under nitrogen. Dichloromethane (CH_2Cl_2) was dried over calcium hydride and was distilled under nitrogen before use. Methanol (MeOH) was distilled under nitrogen. Other organic solvents were used without purification. ^1H (500 MHz), ^{13}C (125.65 MHz), ^{17}O (67.70 MHz), and ^{77}Se (95.35 MHz) NMR spectra were measured at 298 K on a JEOL α500 spectrometer. The sample was dissolved in $CDCl_3$ containing tetramethylsilane as an internal standard for ^1H and ^{13}C NMR. For ^{17}O NMR, D_2O (δ 0.0 ppm) was used as an external standard. For ^{77}Se NMR, dimethyl selenide (δ 0 ppm) in $CDCl_3$ was used as an external standard.

Bis(2-formylphenyl) Diselenide (1e). Bis[2-(hydroxymethyl)phenyl] diselenide (**2e**)[8a] (2.06 g, 5.5 mmol) was dissolved in dimethyl sulfoxide (6 mL) under nitrogen atmosphere. To the solution was added trimethylsilyl chloride (3.5 mL, 27.6 mmol). After 15 min, the reaction was worked up with aqueous sodium hydrogencarbonate, and the mixture was extracted with CH_2Cl_2. The organic layer was collected, dried over anhydrous sodium sulfate, filtrated, and then evaporated. The resulting crude product was purified by silica gel column chromatography (benzene) to yield **1e** (1.05 g, 52%) as slightly yellow crystals. Spectral data for **1e**: ^1H NMR δ 10.17 (s, 2H), 7.87−7.80 (m, 4H), 7.44−7.39 (m, 4H); ^{13}C NMR δ 192.9, 135.9, 134.8, 134.6, 134.4, 131.1, 126.3; ^{77}Se NMR δ 458.5. Anal. Calcd for $C_{14}H_{10}O_2Se_2$: C, 45.68; H, 2.74. Found: C, 45.43; H, 2.82.

^{17}O-Labeled Bis(2-formylphenyl) Diselenide (1e*). To a 45.6 mM *p*-dioxane solution of **1e** (60 mL, 2.74 mmol) were added a 20:1 v/v mixture (1.04 mL) of ^{17}O-labeled hydrogen oxide (21.89 at. % $H_2{}^{17}O$; CDN Isotope, Inc.) and concentrated hydrochloric acid (36%, 11.85 M) under nitrogen atmosphere. After being stirred for 17 h at 30 °C, the reaction mixture was evaporated in vacuo. ^{17}O-labeled **1e*** was obtained in spectrally pure form (1.00 g, 99% yield). Spectral data for **1e***: ^{17}O NMR δ 559.3 (broad s).

2-Formylbenzeneselenenyl Chloride (1a). Compound **1e** (25.8 mg, 0.07 mmol) was dissolved in dry THF (3 mL) under nitrogen. To the solution was added sulfuryl chloride (6.8 μL, 0.08 mmol). After being stirred for 1 h at room temperature, the reaction mixture was concentrated under reduced pressure. The residual brown oil was pure **1a** according to the ^1H, ^{13}C, and ^{77}Se NMR spectra. Spectral data for **1a**: ^1H NMR δ 10.27 (s, 1H), 8.24 (d, J = 8.0 Hz, 1H), 8.09 (dd, J = 8.0 and 1.5 Hz, 1H), 7.78 (td, J = 8.0 and 1.5 Hz, 1H), 7.51 (t, J = 8.0 Hz, 1H); ^{13}C NMR δ 192.5, 148.7, 135.7, 133.6, 132.7, 127.4, 126.1; ^{77}Se NMR δ 1114.1 (lit. 1097[28]). A similar procedure was applied to **1e*** for the synthesis of ^{17}O-labeled **1a** (**1a***). Spectral data for **1a***: ^{17}O NMR δ 493.0 (broad s).

2-Formylbenzeneselenenyl Bromide (1b). Compound **1e** (27.9 mg, 0.08 mmol) was dissolved in CH_2Cl_2 (3 mL) under nitrogen. To the solution was added bromine (4.0 μL, 0.08 mmol). After 15 min, the reaction mixture was evaporated. The residual brown solid was pure **1b** according to the ^1H, ^{13}C, and ^{77}Se NMR spectra. Spectral data for **1b**: ^1H NMR δ 10.12 (s, 1H), 8.19 (d, J = 8.4 Hz, 1H), 8.01 (dd, J = 8.4 and 1.5 Hz, 1H), 7.72 (td, J = 8.4 and 1.5 Hz, 1H), 7.51 (t, J = 8.4 Hz, 1H); ^{13}C NMR δ 192.4, 144.0, 135.6, 134.0, 133.1, 130.4, 126.2; ^{77}Se NMR δ 1029.5 (lit. 1019[28]). A similar procedure was applied to **1e*** for the synthesis of ^{17}O-labeled **1b** (**1b***). Spectral data for **1b***: ^{17}O NMR δ 515.9 (broad s).

2-Formylbenzeneselenenyl Cyanate (1c). Compound **1a**, prepared from **1e** (33.7 mg, 0.09 mmol), was dissolved in dry THF (3.7 mL) under nitrogen. To the solution was added cyanotrimethylsilane (120 μL, 0.91 mmol). After 2 h, the reaction mixture was concentrated under reduced pressure. Product **1c** was obtained in 84% yield (32.3 mg) as a colorless oil after purification of the crude product by silica gel column chromatography (CH_2Cl_2). Spectral data for **1c**: ^1H NMR δ 10.07 (s, 1H), 8.03 (d, J = 8.2 Hz, 1H), 7.93 (dd, J = 8.2 and 1.4 Hz, 1H), 7.68 (td, J = 8.2 and 1.4 Hz, 1H), 7.60 (t, J = 8.2 Hz, 1H); ^{13}C NMR δ 192.8, 135.7, 135.6, 132.6, 130.3, 129.8, 127.8, 104.2; ^{77}Se NMR δ 426.7 (lit. 423[28]). Anal. Calcd for C_8H_5NOSe: C, 45.74; H, 2.40; N, 6.67. Found: C, 45.77; H, 2.51; N 6.79. A similar procedure was applied to **1e*** for the synthesis of ^{17}O-labeled **1c** (**1c***). Spectral data for **1c***: ^{17}O NMR δ 548.0 (broad s).

2-Formylbenzeneselenenyl Phenyl Sulfide (1d). Compound **1e** (54.9 mg, 0.15 mmol) was dissolved in CH_2Cl_2 (6 mL). To the solution were added pyridine (3 drops) and benzenethiol (76.5 μL, 0.75 mmol). After 3 d, the reaction mixture was concentrated under reduced pressure to afford a yellow oil, which contained **1d**, **1e**, and diphenyl disulfide. The yield of **1d** was 78% according to the integration of ^1H NMR. Due to the disproportionation of **1d**, purification could not be performed. Spectral data for **1d**: ^1H NMR δ 10.12 (s, 1H), 8.21 (d, J = 7.1 Hz, 1H), 7.87 (dd, J = 7.1 and 1.3 Hz, 1H), 7.56 (td, J = 7.1 and 1.3 Hz, 1H), 7.48 (dd, J = 7.1 and 1.3 Hz, 2H), 7.43 (td, J = 7.1 and 1.3 Hz, 1H), 7.22 (d, J = 7.1 Hz, 2H), 7.16 (tt, J = 7.1 and 1.3 Hz, 1H); ^{13}C NMR δ 193.0, 138.6, 135.9, 135.6, 134.4, 134.2, 129.1, 129.0, 127.9, 126.8, 126.2; ^{77}Se NMR δ 621.7. A similar procedure was applied to **1e*** for the synthesis of ^{17}O-labeled **1d** (**1d***). Spectral data for **1d***: ^{17}O NMR δ 556.6 (broad s).

2-Formylphenyl Methyl Selenide (1f). To a dimethyl sulfoxide (0.5 mL) solution of potassium hydroxide (18.0 mg, 0.32 mmol) were added compound **1e** (30.5 mg, 0.08 mmol) and methyl iodide (21 μL, 0.34

(28) Llabrès, G.; Baiwir, M.; Piette, J.-L.; Christiaens, L. *Org. Magn. Reson.* **1981**, *15*, 152−154.

mmol) under nitrogen. After 2 h, the reaction was worked up with water, and the mixture was extracted with CH_2Cl_2. Product **1f** was obtained as a colorless oil (16.2 mg, 82%) after purification of the crude product by silica gel column chromatography (benzene). Spectral data for **1f**: ^{1}H NMR δ 10.15 (s, 1H), 7.81 (dd, J = 7.7 and 1.6 Hz, 1H), 7.50 (td, J = 7.7 and 1.6 Hz, 1H), 7.46 (d, J = 7.7 Hz, 1H), 7.35 (td, J = 7.7 and 1.6 Hz, 1H), 2.30 (s, 3H); ^{13}C NMR δ 192.4, 138.6, 135.4, 134.2, 133.7, 127.8, 124.8, 5.8; ^{77}Se NMR δ 259.5 (lit. 267[28]). Anal. Calcd for C_8H_8OSe: C, 48.26; H, 4.05. Found: C, 48.47; H, 4.11. A similar procedure was applied to **1e*** for the synthesis of ^{17}O-labeled **1f** (**1f***). Spectral data for **1f***: ^{17}O NMR δ 561.6 (broad s).

^{17}O-Labeled Bis[2-(hydroxymethyl)phenyl] Diselenide (2e*). ^{17}O-labeled **1e** (**1e***) (56.2 mg, 0.15 mmol) was dissolved in MeOH (3 mL) under nitrogen. To the solution was added sodium borohydride (174 mg, 4.6 mmol). The reaction mixture was stirred under nitrogen for 2h and then under air overnight. The reaction was worked up with aqueous sodium hydrogencarbonate, and the mixture was extracted with CH_2Cl_2. The organic layer was collected, dried over anhydrous sodium sulfate, filtrated, and then evaporated. Product **2e*** (54.9 mg, 97%) was obtained as yellow crystals in pure form, which was confirmed by comparison of the NMR spectra with those of **2e**.[8a] Spectral data for **2e**: ^{1}H NMR δ 7.68 (d, J = 7.5 Hz, 2H), 7.39 (d, J = 7.5 Hz, 2H), 7.31 (t, J = 7.5 Hz, 2H), 7.20 (t, J = 7.5 Hz, 2H), 4.73 (s, 4H); ^{13}C NMR δ 142.1, 135.0, 130.6, 128.9, 128.8, 128.4, 65.3; ^{77}Se NMR δ 433.2. Anal. Calcd for $C_{14}H_{14}O_2Se_2$: C, 45.18; H, 3.79. Found: C, 44.88; H, 3.72. Spectral data for **2e***: ^{17}O NMR δ 13.3 (broad s).

2-(Hydroxymethyl)benzeneselenenyl Chloride (2a). Compound **2a** was prepared from diselenide **2e** quantitatively following the synthetic procedure of **1a**. Brown oil. Spectral data for **2a**: ^{1}H NMR δ 7.78 (broad m, 1H), 7.34 (broad m, 1H), 7.21 (broad m, 2H), 4.84 (broad s, 2H), 2.95 (broad s, 1H); ^{13}C NMR δ 134.3, 130.0, 129.0, 127.1, 127.0, 125.9, 66.9; ^{77}Se NMR δ 987.1. Spectral data for ^{17}O-labeled **2a** (**2a***): ^{17}O NMR δ 24.9 (broad s).

2-(Hydroxymethyl)benzeneselenenyl Bromide (2b). Compound **2b** was prepared from diselenide **2e** quantitatively following the synthetic procedure of **1b**. Brown oil. Spectral data for **2b**: ^{1}H NMR δ 7.85 (broad d, J = 7.0 Hz, 1H), 7.34−7.22 (broad m, 3H), 4.85 (broad s, 2H), 2.39 (broad s, 1H); ^{13}C NMR, signals not observed due to significant line broadening; ^{77}Se NMR δ 839.5. Spectral data for ^{17}O-labeled **2b** (**2b***): ^{17}O NMR δ 23.2 (broad s).

2-(Hydroxymethyl)benzeneselenenyl Cyanate (2c). Compound **2c** was prepared from diselenide **2e** in 72% yield following the synthetic procedure of **1c**. Colorless oil. Spectral data for **2c**: ^{1}H NMR δ 7.85−7.82 (m, 1H), 7.32−7.27 (m, 2H), 7.23−7.20 (m, 1H), 4.71 (s, 2H); ^{13}C NMR δ 139.5, 131.7, 129.4, 128.0, 127.8, 124.8, 104.7, 65.3; ^{77}Se NMR δ 314.5. Anal. Calcd for C_8H_7NOSe: C, 45.30; H, 3.33; N, 6.60. Found: C, 45.26; H, 3.49; N 6.41. Spectral data for ^{17}O-labeled **2c** (**2c***): ^{17}O NMR δ 22.0 (broad s).

2-(Hydroxymethyl)benzeneselenenyl Phenyl Sulfide (2d). Compound **2b**, prepared from diselenide **2e** (31.1 mg, 0.08 mmol) and bromine (4.3 μL, 0.08 mmol), was dissolved in CH_2Cl_2 (3.5 mL). To the solution were added pyridine (2 drops) and benzenethiol (19.0 μL, 0.19 mmol). After 1 h, the reaction mixture was concentrated under reduced pressure to afford a yellow oil, which contained **2d**, **2e**, and diphenyl disulfide. The yield of **2d** was 25% according to the integration of ^{1}H NMR. Due to the disproportionation of **2d**, purification could not be performed. Spectral data for **2d**: ^{1}H NMR δ 7.73 (d, J = 8.5 Hz, 1H), 7.46 (d, J = 8.5 Hz, 2H), 7.35 (d, J = 8.5 Hz, 1H), 7.23−7.18 (m, 5H), 4.77 (s, 2H); ^{13}C NMR δ 140.4, 136.2, 132.4, 130.2, 129.5, 128.8, 128.4, 127.5, 127.2, 127.1, 64.5; ^{77}Se NMR δ 501.8. A similar procedure was applied to **2e*** for the synthesis of ^{17}O-labeled **2d** (**2d***). Spectral data for **2d***: ^{17}O NMR δ 16.0 (broad s).

2-(Hydroxymethyl)phenyl Methyl Selenide (2f). Compound **2e** (24.7 mg, 0.07 mmol) and methyl iodide (20 μL, 0.32 mmol) were dissolved in MeOH (2 mL) under nitrogen. To the solution was added sodium borohydride (170 mg, 4.5 mmol). After 2 h, the reaction was worked up with aqueous sodium hydrogencarbonate, and the mixture was extracted with CH_2Cl_2. Product **2f** was obtained as a colorless oil (25.6 mg, 96%). Spectral data for **2f**: ^{1}H NMR δ 7.43−7.40 (m, 1H), 7.36−7.33 (m, 1H), 7.24−7.20 (m, 2H), 4.72 (s, 2H), 2.40 (s, 1H), 2.31 (s, 3H); ^{13}C NMR δ 140.8, 131.5, 130.6, 128.4, 128.0, 126.5, 7.3; ^{77}Se NMR δ 157.2. Anal. Calcd for $C_8H_{10}OSe$: C, 47.77; H, 5.01. Found: C, 47.71; H, 5.08. A similar procedure was applied to **2e*** for the synthesis of ^{17}O-labeled **2f** (**2f***). Spectral data for **2f***: ^{17}O NMR δ 10.6 (broad s).

2-(Isopropoxymethyl)phenyl Isopropyl Selenide (4). To a dimethyl sulfoxide (32 mL) solution of potassium hydroxide (3.60 g, 64 mmol) were added compound **2e** (743 mg, 2.0 mmol) and isopropyl bromide (6.0 mL, 64 mmol) under nitrogen. After 20 h, isopropyl bromide (6.0 mL, 64 mmol) was added again to the solution. The mixture was stirred for another 20 h. The reaction was worked up with water, and the mixture was extracted with ether. Product **4** was obtained as a colorless oil (508 mg, 47%) after purification of the crude product by silica gel column chromatography (CH_2Cl_2). Spectral data for **4**: ^{1}H NMR δ 7.55 (dd, J = 7.9 and 1.1 Hz, 1H), 7.46 (dd, J = 7.9 and 1.1 Hz, 1H), 7.27 (td, J = 7.9 and 1.1 Hz, 1H), 7.18 (td, J = 7.9 and 1.1 Hz, 1H), 4.63 (s, 2H), 3.72 (sep, J = 6.2 Hz, 1H), 3.47 (sep, J = 6.2 Hz, 1H), 1.41 (d, J = 6.2 Hz, 6H), 1.23 (d, J = 6.2 Hz, 6H); ^{13}C NMR δ 141.4, 134.7, 130.4, 128.5, 127.8, 127.4, 71.2, 70.3, 33.6, 24.1, 22.2; ^{77}Se NMR δ 368.5. Anal. Calcd for $C_{13}H_{20}OSe$: C, 57.56; H, 7.43. Found: C, 57.64; H, 7.39. A similar procedure was applied to **2e*** for the synthesis of ^{17}O-labeled **4** (**4***). Spectral data for **4***: ^{17}O NMR δ 39.0 (broad s).

Bis[2-(isopropoxymethyl)phenyl] Diselenide (3e). Compound **4** (465 mg, 1.7 mmol) was dissolved in MeOH. To the solution was added 30% hydrogen peroxide (1.5 mL, 15 mmol). After being stirred under air for 17 h, the reaction mixture was evaporated in vacuo. The organic residue was dissolved in dry THF (35 mL), and to the solution was added lithium aluminum hydride (672 mg, 18 mmol). After having refluxed for 2 h, the reaction was worked up with 2 M hydrochloric acid (50 mL), and the mixture was extracted with ether (50 mL). Product **3e** was obtained as a yellow oil (229 mg, 59%) after purification of the crude product by silica gel column chromatography (CH_2Cl_2). Spectral data for **3e**: ^{1}H NMR δ 7.75 (dd, J = 7.9 and 1.1 Hz, 2H), 7.30 (dd, J = 7.9 and 1.1 Hz, 2H), 7.20 (td, J = 7.9 and 1.1 Hz, 2H), 7.17 (td, J = 7.9 and 1.1 Hz, 2H), 4.58 (s, 2H), 3.72 (sep, J = 6.2 Hz, 2H), 1.23 (d, J = 6.2 Hz, 12H); ^{13}C NMR δ 138.7, 132.4, 131.8, 128.7, 128.3, 127.2, 71.4, 70.5, 22.1; ^{77}Se NMR δ 412.0. Anal. Calcd for $C_{20}H_{26}O_2Se_2$: C, 52.64; H, 5.74. Found: C, 52.53; H, 5.44. A similar procedure was applied to **4*** for the synthesis of ^{17}O-labeled **3e** (**3e***). Spectral data for **3e***: ^{17}O NMR δ 39.0 (broad s).

2-(Isopropoxymethyl)benzeneselenenyl Chloride (3a). Compound **3a** was prepared from diselenide **3e** quantitatively following the synthetic procedure of **1a**. Brown oil. Spectral data for **3a**: ^{1}H NMR δ 7.77 (d, J = 7.7 Hz, 1H), 7.34 (td, J = 7.7 and 2.3 Hz, 1H), 7.20−7.16 (m, 2H), 4.61 (s, 2H), 3.81 (sep, J = 6.2 Hz, 1H), 1.27 (d, J = 6.2 Hz, 6H); ^{13}C NMR δ 136.0, 134.6, 129.0, 128.0, 126.4, 126.1, 73.1, 71.0, 21.9; ^{77}Se NMR δ 986.5. Spectral data for ^{17}O-labeled **3a** (**3a***): ^{17}O NMR δ 54.8 (broad s).

2-(Isopropoxymethyl)benzeneselenenyl Bromide (3b). Compound **3b** was prepared from diselenide **3e** quantitatively following the synthetic procedure of **1b**. Brown oil. Spectral data for **3b**: ^{1}H NMR δ 7.82 (d, J = 7.7 Hz, 1H), 7.30 (td, J = 7.7 and 1.7 Hz, 1H), 7.20 (t, J = 7.7 Hz, 1H), 7.16 (dd, J = 7.7 and 1.7 Hz, 1H), 4.60 (s, 2H), 3.80 (sep, J = 6.2 Hz, 1H), 1.26 (d, J = 6.2 Hz, 6H); ^{13}C NMR δ 136.9, 132.1, 131.3, 129.1, 126.8, 126.7, 72.6, 71.0, 22.0; ^{77}Se NMR δ 857.8. Spectral data for ^{17}O-labeled **3b** (**3b***): ^{17}O NMR δ 55.2 (broad s).

2-(Isopropoxymethyl)benzeneselenenyl Cyanate (3c). Compound **3c** was prepared from diselenide **3e** in 97% yield following the synthetic procedure of **1c**. Colorless oil. Spectral data for **3c**: ^{1}H NMR δ 7.83 (dd, J = 7.5 and 1.3 Hz, 1H), 7.34−7.25 (m, 3H), 4.51 (s, 2H), 3.71 (sep, J = 6.2 Hz, 1H), 1.23 (d, J = 6.2 Hz, 6H); ^{13}C NMR δ 137.7,

131.6, 129.7, 128.8, 128.0, 125.4, 104.6, 71.8, 70.0, 21.8; ^{77}Se NMR δ 315.1. Anal. Calcd for $C_{11}H_{13}NOSe$: C, 51.98; H, 5.15; N, 5.51. Found: C, 51.94; H, 5.07; N, 5.58. Spectral data for ^{17}O-labeled **3c** (**3c***): ^{17}O NMR δ 44.6 (broad s).

2-(Isopropoxymethyl)benzeneselenenyl Isopropyl Sulfide (3d). Compound **3d** was prepared from diselenide **3e** following the synthetic procedure of **2d**. Product **3d** was obtained as a mixture with **3e** and diphenyl disulfide due to the disproportionation. The yield of **3d** was 48% according to the integration of ^{1}H NMR. Spectral data for **3d**: ^{1}H NMR δ 7.83−7.15 (m, 9H), 4.56 (s, 2H), 3.73 (sep, J = 6.2 Hz, 1H), 1.24 (d, J = 6.2 Hz, 6H); ^{13}C NMR δ 138.0, 134.7, 133.8, 129.9, 129.1, 128.9, 128.8, 128.4, 127.0, 126.8, 71.4, 70.4, 22.0; ^{77}Se NMR δ 503.8. Spectral data for ^{17}O-labeled **3d** (**3d***): ^{17}O NMR δ 44.4 (broad s).

2-(Isopropoxymethyl)phenyl Methyl Selenide (3f). Compound **3f** was prepared from diselenide **3e** in 52% yield following the synthetic procedure of **1f**. Colorless oil. Spectral data for **3f**: ^{1}H NMR δ 7.39 (dd, J = 7.2 and 1.5 Hz, 1H), 7.36 (dd, J = 7.2 and 1.5 Hz, 1H), 7.22 (td, J = 7.2 and 1.5 Hz, 1H), 7.19 (td, J = 7.2 and 1.5 Hz, 1H), 4.56 (s, 2H), 3.73 (sep, J = 6.2 Hz, 1H), 2.30 (s, 3H), 1.24 (d, J = 6.2 Hz, 6H); ^{13}C NMR δ 138.8, 132.8, 129.7, 128.5, 128.2, 125.9, 71.2, 70.0, 22.1, 6.2; ^{77}Se NMR δ 166.6. Anal. Calcd for $C_{11}H_{16}OSe$: C, 54.32; H, 6.63. Found: C, 54.45; H, 6.70. Spectral data for ^{17}O-labeled **3f** (**3f***): ^{17}O NMR δ 39.0 (broad s).

Computational Methods. All theoretical calculations were carried out by using the Gaussian 98 program[29] except for the atoms in molecules (AIM) analysis. The hybrid Becke 3-Lee−Yang−Parr (B3LYP) exchange-correlation functional[30] was applied for DFT calculations. Huzinaga's 43321/4321/311 basis sets[31] were used for Se and Br, and 6-31G(d,p) basis sets were used for other atoms. The combination is denoted here as 631H basis sets. Geometries were fully optimized at the HF/631H and then B3LYP/631H levels of theory. To save computational time, a phenylthio (SPh) group of compound **d** and an arylseleno (SeAr) group of compound **e** were simplified to a methylthio (SMe) group (in compound **d′**) and a methylseleno (SeMe) group (in compound **e′**), respectively, in calculation. Similarly, an isopropyl group of series **3** was simplified to a methyl group in series **5**. For all stable conformers, the nature as a potential energy minimum was established at the B3LYP/631H level by verifying that all vibrational frequencies were real. The single-point energies were corrected with zero-point energies (ZPE). The orbital interaction energies between Se and O atoms ($E_{Se\cdots O}$) as well as the atomic charges (q_{Se} and q_O) were calculated by using the natural bond orbital (NBO) method[4] at the B3LYP/631H level. The AIM analysis was performed by using the AIM2000 program.[32] Topological properties of the electron density ($\rho_{Se\cdots O}$) at the bond critical points (BCP) of nonbonded Se···O interactions were characterized at the B3LYP/631H level.

Acknowledgment. This work was supported by Grants in Aid for Scientific Research Nos. 11120210 and 10133207 from the Ministry of Education, Science, and Culture, Japan.

JA049690N

(29) Frisch, M. J.; Trucks, G. W.; Schlegel, H. B.; Scuseria, G. E.; Robb, M. A.; Cheeseman, J. R.; Zakrzewski, V. G.; Montgomery, J. A.; Stratmann, R. E.; Burant, J. C.; Dapprich, S.; Millam, J. M.; Daniels, A. D.; Kudin, K. N.; Strain, M. C.; Farkas, O.; Tomasi, J.; Barone, V.; Cossi, M.; Cammi, R.; Mennucci, B.; Pomelli, C.; Adamo, C.; Clifford, S.; Ochterski, J.; Petersson, G. A.; Ayala, P. Y.; Cui, Q.; Morokuma, K.; Malick, D. K.; Rabuck, A. D.; Raghavachari, K.; Foresman, J. B.; Cioslowski, J.; Ortiz, J. V.; Baboul, A. G.; Stefanov, B. B.; Liu, G.; Liashenko, A.; Piskorz, P.; Komaromi, I.; Gomperts, R.; Martin, R. L.; Fox, D. J.; Keith, T.; Al-Laham, M. A.; Peng, C. Y.; Nanayakkara, A.; Gonzalez, C.; Challacombe, M.; Gill, P. M. W.; Johnson, B.; Chen, W.; Wong, M. W.; Andres, J. L.; Gonzalez, C.; Head-Gordon, M.; Replogle, E. S.; Pople, J. A. *Gaussian 98*; Gaussian, Inc.: Pittsburgh, PA, 1998.

(30) (a) Lee, C.; Yang, W.; Parr, R. G. *Phys. Rev. B* **1988**, *37*, 785−789. (b) Becke, A. D. *J. Chem. Phys.* **1993**, *98*, 5648−5652.

(31) *Gaussian Basis Sets for Molecular Calculations*; Huzinaga, S., Ed.; Elsevier: Amsterdam, 1984.

(32) Biegler-König, F.; Schönbohm, J.; Bayles, D. *J. Comput. Chem.* **2001**, *22*, 545−559.